INAF-Osservatorio astrofisico di Torino
Technical Report nr. 165

Coronagraphic WL and UV observations of CMEs: requirements for the development of future instrumentation

A. Bemporad

Pino Torinese, 26 novembre 2013

Coronagraphic WL and UV observations of CMEs: requirements for the development of future instrumentation

A. Bemporad

INAF-Osservatorio Astrofisico di Torino, via Osservatorio 20,
10025 Pino Torinese (TO), Italy; bemporad@oato.inaf.it

ABSTRACT

This report summarizes the typical properties of coronagraphic white light (WL) and UV observations of Coronal Mass Ejections (CMEs), making a list of requirements for the development of future instrumentation like METIS on Solar Orbiter. After a summary (Par. 1) of some of the main new observational capabilities METIS will provide on CME observations, I will give the typical observational properties of CMEs in both WL and UV (focusing only on imaging – and not spectroscopic – properties), first discussing typical WL and UV brightness variations during CMEs (Par. 2), second focusing on other observational properties (Par. 3). Hence, the main requirements for METIS CME observation modes are discussed (Par. 4) and possible CME observational sequences and campaigns are provided (Par. 5). During CMEs the WL increases only by 30%-40%, while UV (HI Lyman-α) intensity is comparable with coronal streamers at solar max, hence with exposure times considered for coronal observations we expect no image saturation during CMEs. If we want to study the small-scale structure of faster CMEs, by assuming a speed by 1200-2200 km/s, with METIS resolutions by 4100-9900 km/2pix, exposure times on the order of ~ 2-8 sec are required. The CME front will leave the METIS FOV in ~ 500-1000 sec at 0.28-0.32 AU and in ~ 1000-2000 sec at 0.68 AU, but to observe the whole event and post-CME reconfiguration up to ~ 4-6 hours of data after CME initiation (trigger) could be required. During the first 2 orbits of Solar Orbiter no more than ~ 2-4 CMEs per day are expected, hence once the CME mode is activated it should last for at least ~ half a day in order to be sure to detect at least one CME. Given observational and instrumental constraints on the exposure times, time cadences, total duration, telemetry rate, etc… possible WL, UV, WL+UV observational sequences and observational campaigns for CMEs are provided.

TABLE OF CONTENTS

LIST OF FIGURES

LIST OF TABLES

1. New scientific capabilities offered by METIS

In what follows I summarize some of the main new capabilities[1] for CMEs observations that will be provided by the future METIS instrument onboard the ESA – Solar Orbiter mission.

- **Out-of-ecliptic stereoscopy**: the coronagraphic channel of METIS will provide the first ever observations of CMEs in white light and EUV from an out-of-ecliptic view (up to a helio-latitude of 34° in the extended mission phase). This will provide the future capability to make 3D stereoscopic observations of CMEs (as those currently provided by the twin STEREO spacecraft) combining one view provided by METIS on Solar Orbiter and a second view provided by the future coronagraphs located on spacecraft in orbit around L1 (such as SOHO) or around the Earth (such as Hinode and SDO), hence on the ecliptic plane. Stereoscopic capability will be also combined with 3D reconstructions performed with polarization ratio technique applied to METIS data acquired in the white light channel with linear polarimeter.

- **Pre- and post-eruption coronal evolution**: around the periods of closest approach, Solar Orbiter will be in quasi-corotation with the Sun for a few days. During corotation the evolution of the pre-CME corona will be sampled without effects related to the solar rotation, thus allowing us to ascertain whether the main source of flux injection into the heliosphere is indeed residing in the outer corona and to identify the mechanism driving the eruption. Moreover, the post-CME evolution will allow us to study the restructuring of the global corona following a mass ejection.

- **Quadrature observations with Solar Probe**: over the last 15 years important information on CMEs have been also derived by a comparison between plasma parameters measured with remote-sensing techniques by SOHO and those measured *in situ* with Ulysses. These comparisons were possible in the so-called quadrature configurations, i.e. when the Ulysses spacecraft crossed the SOHO plane of the sky. Nevertheless, associations of features observed *in situ* at heliocentric distances typically ranging between 2 and 5 AU with those observed in the lower corona (below 0.15 AU) were quite a difficult task, because of the large spatial and temporal intervals separating the two measurements. During the Solar Orbiter mission, quadratures with Solar Probe+ will occur 3-6 times per year, with Solar Probe+ at an average distance of 0.28 AU, and many times with Solar Probe+ closer than 0.1 AU. Hence, CME parameters derived with METIS coronagraphic images in the intermediate corona (between 1.5 and 3.1 solar radii with Solar Orbiter at 0.28 AU) will be easily compared with those measured *in situ* at small heliocentric distances by Solar Probe+, allowing a much better identification of SEP sources and CME-driven shocks properties.

- **Multi-slit studies**: the spectroscopic channel of METIS will provide the first ever multi-slit spectra of CMEs, thanks to its 3 slits placed at a relative distance of 0.3° (corresponding to 0.3 solar radii at the closest approach of 0.28 AU). Spectroscopic observations performed so far with SOHO/UVCS acquired CME spectra sampling the emitting plasma at a fixed altitude as the CME bubble expands outwards. Reconstructed CME images in the EUV emission provided unique information on the plasma temperature and elemental abundance distribution in the CME cores and fronts. Nevertheless, these observations mixed temporal variations of plasma physical parameters related to the CME expansion with those due to spatial inhomogeneities within the expanding eruption. The multi-slit capability provided by METIS will allow for the first time to disentangle between the temporal and spatial evolution of physical parameters such as outflow velocities, neutral H and He^{+}

[1] *All these points were presented during the 4th (March 2011, Telluride CO) and 5th (September 2012, Bruges, BE) Solar Orbiter Meetings. Some of them – the last 3 in particular – refer also to the spectroscopic data and HeII 304Å imaging, which are capabilities no more included in the actual design of METIS instrument after the significant descoping that occurred between December 2012 and September 2013. In any case, these capabilities are listed here for the possible future development of coronagraphic instruments on other solar missions.*

ion kinetic temperatures, He elemental abundances. Moreover, it will be also possible to study in more details the evolution of plasma heating and supra-thermal ions associated with the transit of CME-driven shocks, because the multi-slit spectrometer will provide for some events spectral line broadenings observed at the same time in different positions along the shock-front.

- **HeII 304Å spectroscopy**: HeII 303.78Å "cool" emission from erupting prominences as been observed so far with band-pass telescopes such as SOHO/EIT, Stereo/EUVI and SDO/AIA. Hence, the observed images may also include "hot" component emission from the nearby SiXI 303.32Å line, partially blended with HeII 303.78Å line. Thanks to its spectral resolution by 0.13Å/pixel, METIS will allow for the first time to separate these two spectral lines, thus allowing for the first determination of the SiXI 303.32Å contribution to the observed HeII 303.78Å band-pass images. Moreover, a measure of EUV emission in the resonance H and He lines can also be used to estimate the radial velocity component with the Doppler dimming technique and, in combination with line of sight velocity provided by Doppler shifts, to infer the full 3D velocity vector of the erupting prominence.

- **HeII 304Å imaging**: observations acquired over the last decades demonstrate that many (but not all) CMEs result from a filament/prominence eruption, usually observed in the low corona (i.e. below ~0.4 solar radii off-limb) as expanding tongues of plasma emitting in the HeII 304Å line (corresponding to ~10^4-10^5 K) immersed into EUV cavities which are typically delimited by semicircular loop-like expanding features emitting in the FeXII 195Å line and other coronal lines (~10^6 K). UVCS observations demonstrated that the prominence plasma form at higher altitudes the CME core, resulting in EUV emission of cool lines (e.g. CIII 977 Å, SiIII 1206Å). Unexpectedly, UVCS also observed signatures of high temperature emissions in the CME core and demonstrate that for many event a significant plasma heating is required at the core in order to reproduce the observations. Source for this additional heating is at present unknown. METIS will provide the first ever coronagraphic images of CMEs in the HI 1216Å and HeII 304Å spectral lines, thus allowing us to study the evolution of the prominence material temperatures in the intermediate corona (above 1.5 solar radii).

Given the above capabilities, in what follows I give the typical observational properties of CMEs in both WL and UV (focusing only on imaging – and not spectroscopic – properties), first discussing typical WL and UV brightness variations during CMEs (Par. 2), second focusing on other observational properties (Par. 3). Hence, the main requirements for METIS CME observation modes are discussed (Par. 4) and possible CME observational sequences and campaigns are provided (Par. 5).

2. Relative variations of WL (tB and pB) and UV (HI Lyman-α) during CMEs

This paragraph summarizes the main WL and UV intensity variations expected in coronagraphic images during the occurrence of CMEs[2]. Relative variations of WL total (i.e. unpolarized) intensity tB during CMEs have been investigated with SOHO/LASCO C2 data, while relative variations of WL polarized brightness (pB) have been studied with STEREO/COR1 data. Reason is that typically LASCO/C2 acquires only 2 pB images per day, hence it is really hard to have a pB image of a CME with LASCO, while COR1 routinely acquires every day sequences of 3 images with 3 different orientations of the polarizer every 5 minutes, hence providing a pB image every 5 minutes. The approximate start times of the selected events (as listed in the LASCO and STEREO CME catalogs) are reported in Table 1.

[2] *All the information provided here have been sent to the METIS PO on 12/11/2012 for the METIS document on coronal radiances.*

LASCO/C2 events:	STEREO/COR1 events:
11/06/1999, 11:26 UT	07/06/2011, 06:49 UT
08/11/2000, 19:27 UT	09/02/2012, 20:25 UT
08/11/2000, 23:06 UT	24/03/2012, 00:10 UT
21/08/2001, 12:06 UT	
28/06/2005, 17:06 UT	

Table 1: list of WL events selected and analyzed in this report.

For each one of the events listed in Table 1 I downloaded, calibrated and analyzed 1 pre-CME coronal image and 1 – 3 images during the CME (depending on the duration of each event). For each event the total (tB) and polarized (pB) brightness have been extracted before and during the CME along radials centered on the approximate CME central latitude. For each event, the relative variations of the VL brightness during CME with respect to the pre-CME corona have been simply computed as $(tB_{CME} - tB_{pre})/tB_{pre}$ and $(pB_{CME} - pB_{pre})/pB_{pre}$. Resulting peak values and radially averaged values of tB and pB variations during CMEs are reported in Table 2.

VL Relative variations from LASCO/C2 data						
Time (UT)	peak value (tB, %)	peak altitude (tB, R_{sun})	average (2-6 R_{sun})			
11/06/1999, 11:25	24.2	2.27	1.91			
11/06/1999, 11:49	35.8	3.48	14.8			
08/11/2000, 23:27	70.5	3.62	24.8			
08/11/2000, 23:27	37.3	4.37	5.54			
21/08/2001, 12:27	22.7	2.57	3.35			
21/08/2001, 12:50	23.0	2.83	6.98			
21/08/2001, 13:27	17.8	4.33	9.82			
28/06/2005, 17:06	22.9	2.76	3.09			
28/06/2005, 17:30	32.9	2.73	12.3			
28/06/2005, 17:54	24.4	3.49	13.3			
VL Relative variations from STEREO/COR1 data						
Time (UT)	peak value (tB, %)	peak altitude (tB, R_{sun})	average (1.5-4 R_{sun})	peak value (pB, %)	peak altitude (pB, R_{sun})	average (1.5-4 R_{sun})
07/06/2011, 07:30	194	2.13	19.7	1564	2.12	105
09/02/2012, 21:00	14.5	1.81	0.59	240	3.92	5.22
24/03/2012, 00:20	2.05	1.82	0.53	191	2.99	37.1

Table 2: peak values and radially averaged values of tB and pB variations during CMEs as observed with SOHO/LASCO and STEREO/COR1 instruments.

Notice that, because the above values refer only to relative variations (so, no absolute values are provided) of the total and polarized brightness in the VL channel, possible differences due to different calibrations of LASCO and STEREO instruments are removed doing the ratio. Table 2 shows that:

1) relative variations of tB are in general quite small (typically below ~ 30-40%);
2) relative variations of pB are in general quite large (up to a factor ~ 16);
3) relative pB variations are up to ~ 90 times larger than relative tB variations.

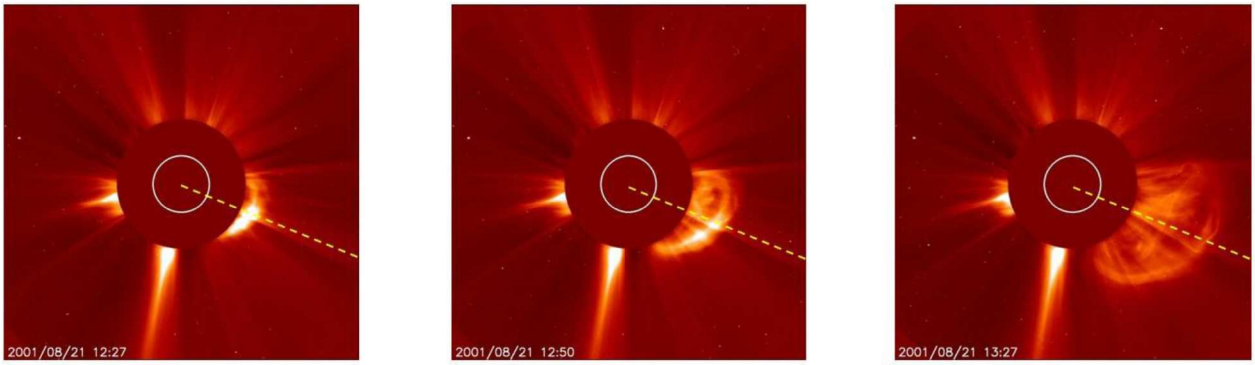

Figure 1: example of LASCO/C2 image sequence acquired during the August 21, 2001 CME at 12:27 (left), 12:50 (middle) and 13:27 (right) UT. Yellow solid line is shown for future reference (see Figure 2).

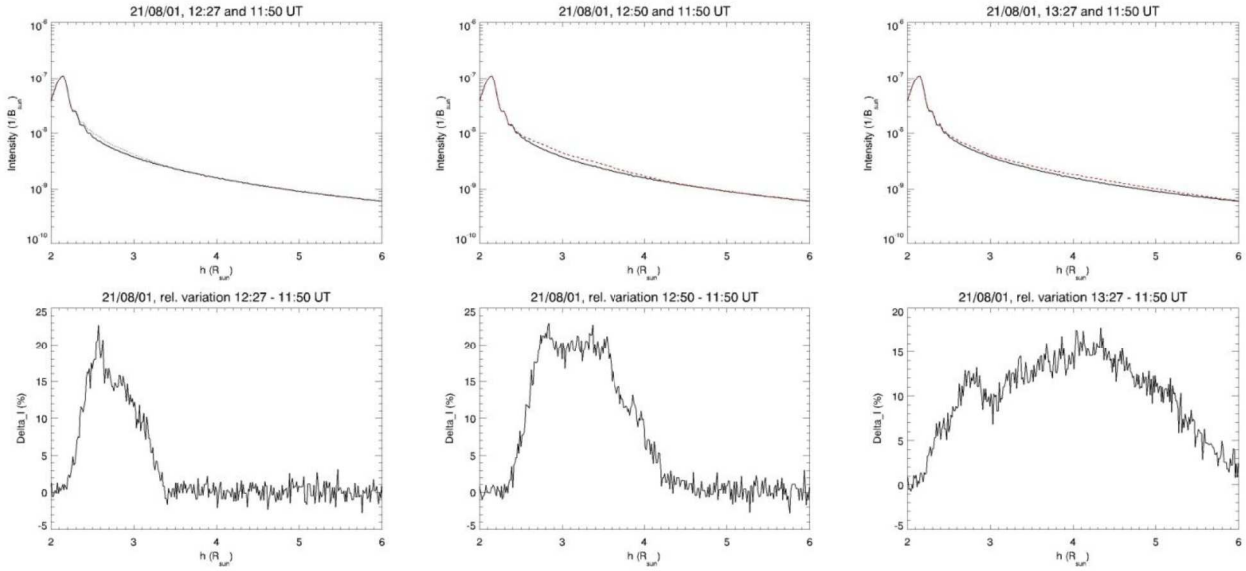

Figure 2, top row radial tB intensity profile along the yellow dashed line shown in Figure 1 before (solid) and during (dotted) the CME. Bottom row: corresponding relative variation of tB.

Relative variations of UV intensities during CMEs have been recently described by Giordano et al. (2013), and main results regarding the CME intensity in UV are just summarized here. In particular, the average HI Lyman-α 1216Å intensities observed for all the events detected by the SOHO/UVCS instrument are provided in Figure 4 as a function of the heliocentric distance of observation: at almost all heights, the H I Lyman-α CME intensity can reach values more than 2 orders of magnitude higher than the values detected in solar maximum streamers at the same heights. Nevertheless, the majority of events have intensities below those typical for coronal streamers at the maximum of solar activity cycle; therefore, they are detected in intensity only by running difference time series. The brightest events are those associated with prominence eruptions, leading to a strong and localized H I Lyman-α emission in the UVCS slit due to the transit of the cool prominence material in the instrument field of view. Unfortunately, statistical distribution of relative variations during CMEs with respect to the pre-CME corona is not provided in the paper.

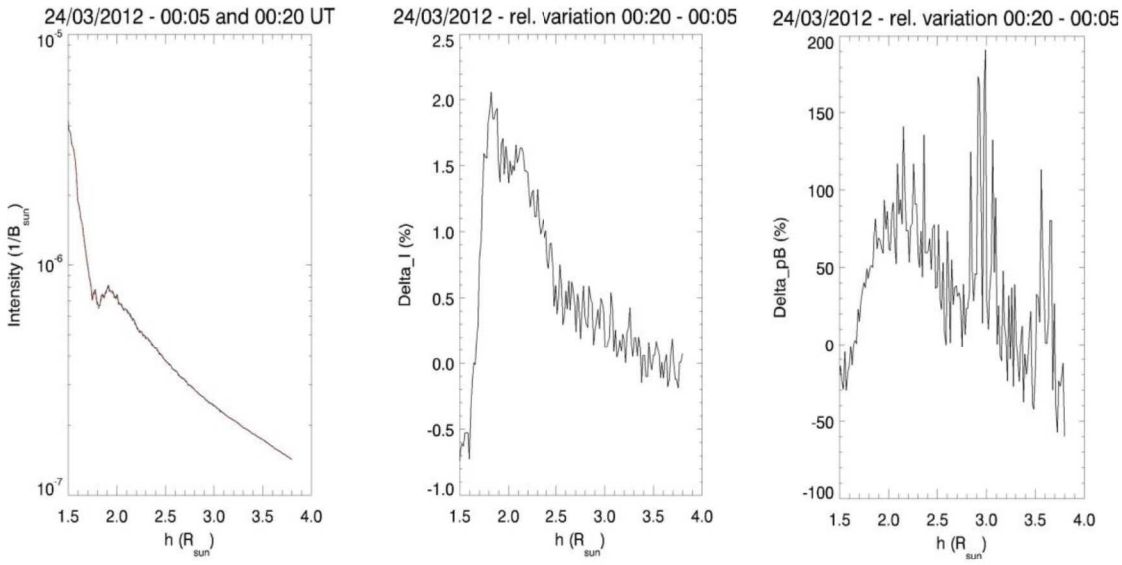

Figure 3, left: example of STEREO/COR1 tB radial profile observed during the March 24, 2012 CME. Middle: corresponding relative variation of tB. Right: corresponding relative variation of pB.

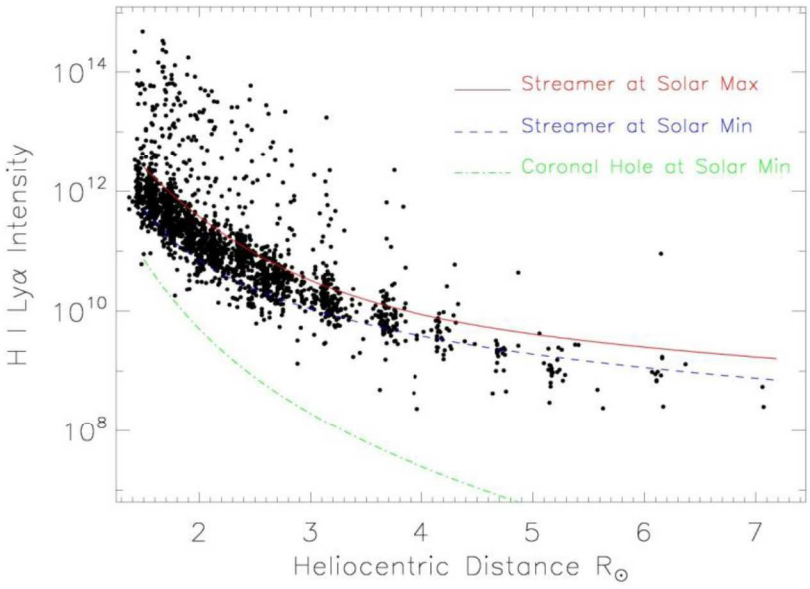

Figure 4: CME intensities in H I Lyman-α 1216Å as a function of the heliocentric heights. For comparison, intensities measured in streamer at solar maximum and minimum and in coronal hole are also plotted (from Giordano et al. 2013).

In summary, during CMEs the WL increases only by 30%-40%, while UV (HI Lyman-α) intensity is comparable with coronal streamers at solar max. This means that with exposure times considered for typical METIS observations for solar corona we expect no image saturation during CMEs.

3. CME other observational properties in WL and UV images

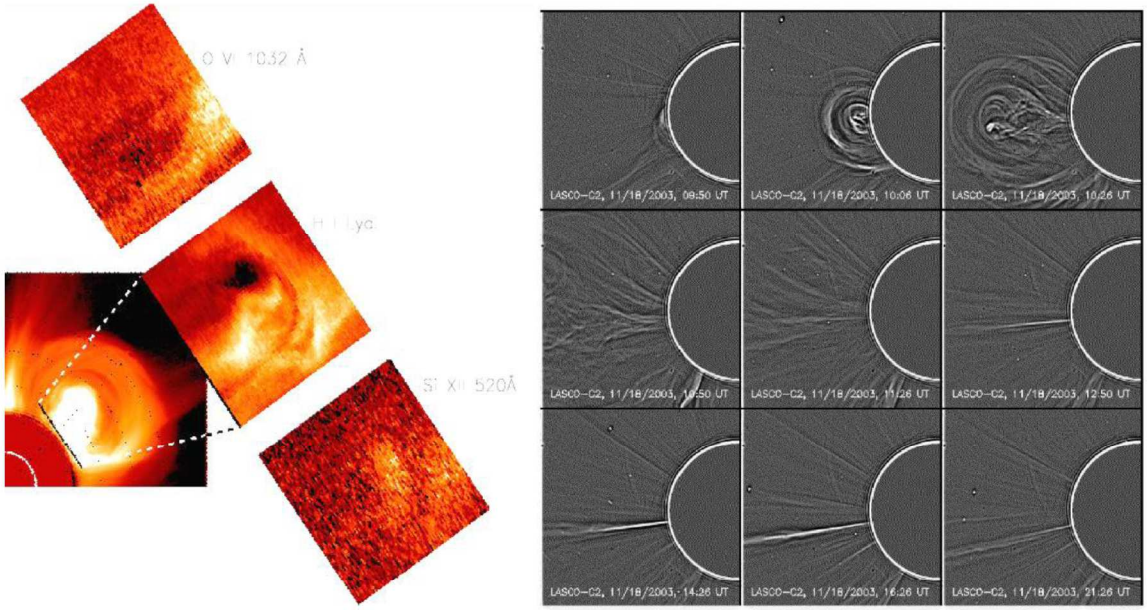

Figure 5: typical CME morphologies as observed in UV (left, from Ciaravella et al. 2003) and WL (right, from Lin et al. 2005) intensities. Contrast in WL images has been enhanced with Wavelet filtering.

This paragraph shortly revise other CME observational properties of interest for the development of a coronagraph[3]. The evolution of UV intensities during CMEs is mainly known thanks to the observations acquired by the SOHO/UVCS spectrometer. UVCS typically observed CMEs with temporal resolutions not smaller than 100s (corresponding to a travel distance by ~ 5×10^4 km for a 500 km/s CME, corresponding to ~ 70") and spatial resolutions not smaller than 3 bins (corresponding to 21", hence ~ 1.5×10^4 km at 1 AU). This means that UV observations of CMEs have spatial resolutions not smaller than a few 70"×21", which is quite a big area if compared with typical resolution for WL coronagraphic observations (see below). For this reason, we actually don't know if CMEs have a fine structure in UV.

On the other hand, WL images of CMEs were acquired much higher spatial resolution (11"×11" for SOHO/LASCO-C2, 4"×4" for STEREO/COR1) and short exposure times (a few seconds): resulting WL images often show small scale filamentary structures embedded in CMEs whose detection is very important to probe the magnetic topology associated with these phenomena. The detection of this small scale filamentary structures has proven to be easily enhanced by image filtering procedures (like those based on the Wavelet transforms).

[3] *All the information provided here were already shown and discussed with the METIS PO with a ppt presentation given on 29/01/2013.*

Coronagraph	OSO-7	Skylab	Solwind	SMM[a]	LASCO[b]
Epoch	1971	1973–74	1979–85	1980, 84–89	1996–present
FOV ($R_\odot$)	2.5–10	1.5–6	3–10	1.6–6	1.2–32
Total # CMEs	27	115	1607	1351	> 10000
Speed (km s^{-1})	–	470	460	349	489
Acceleration (m s^{-2})	–	–	–	–	–16 to +5
Width (°)	–	42	43	46	47
Mass (10^{15}) g[c]	–	6.2	1.7	3.3	1.3
KE (10^{30}) erg[c]	–	–	4.3	8.0	2.0
Mech. E (10^{30}) erg[c]	–	–	–	–	4.2

Table 3: average statistical properties of CMEs as observed in WL by different solar missions (from Webb & Howard 2012).

Table 1
All High-Speed CMEs (V > 1500 km s^{-1}) Between 1997 and 1999

Event	CME Date	First Appearance (C2 UT)	Linear Speed (km s^{-1})	AW (deg)	P.A. (deg)	Type II (Dm)
1	1997 Nov 6	12:10:00	1556	360	262	Yes
2	1998 Mar 31	6:12:00	1992	360	177	No
3	1998 Apr 20	10:07:00	1863	165	278	Yes
4	1998 Apr 23	5:27:00	1618	360	116	Yes
5	1998 May 9	3:35:58	2331	178	262	Yes
6	1998 Jun 4	2:04:00	1802	360	314	No
7	1998 Nov 24	2:30:00	1798	360	226	No
8	1998 Nov 26	6:18:05	1505	360	198	No
9	1998 Dec 18	18:21:00	1749	360	36	Yes
10	1999 May 3	6:06:00	1584	360	88	Yes
11	1999 May 27	11:06:00	1691	360	341	Yes
12	1999 Jun 1	19:37:00	1772	360	359	Yes
13	1999 Jun 4	7:26:54	2230	150	289	Yes
14	1999 Jun 11	11:26:00	1569	181	38	Yes
15	1999 Sep 11	21:54:00	1680	120	13	No

Table 4: typical CME speeds measured for events associated with a clear CME driven shock visible in WL data (from Ontiveros & Vourlidas 2009)

Obviously, the exposure times needed to resolve these features depend on two main parameters: 1) the coronagraph (METIS) spatial resolution and 2) the average CME velocities. Typical CME speeds as observed by previous solar missions are summarized in Tables 3 and 4: on average CMEs have a projected speeds around 350 – 470 km/s, but only those with much higher speeds around 1600 – 2200 km/s show also a clear WL signature of CME-driven shocks. According to this fact, CME speeds for events were also a type-II or type-III radio emission is observed are on average on the order of ~1200-1500 km/s, as summarized in the recent review by Gopalswamy et al. (2010).

METIS FOV during SolO Mission (reference trajectory: Jan 2017 launch, trajectory file 2017_January_CReMA_Issue2-1.oem)								
	SolO Orbit. Nmbr.	Distance (AU)	FOV_down (Rsun)	FOV_up (Rsun)	Latitude (deg)	Time (days)	Time (years)	Time (UT)
CRUISE PHASE	1							
		0,509	2,86	5,54	14,15	529,2	1,45	2018-06-14T08:15:24.13781455
		0,482	2,71	5,24	11,19	540,2	1,48	2018-06-25T08:15:24.13781455
		0,930	5,23	10,13	-14,16	614,2	1,68	2018-09-07T08:15:24.13781455
	2							
		0,511	2,88	5,57	14,16	772,5	2,11	2019-02-12T08:15:24.13781455
		0,482	2,71	5,24	10,93	784,5	2,15	2019-02-24T08:15:24.13781455
		0,932	5,25	10,15	-14,16	858,5	2,35	2019-05-09T08:15:24.13781455
	3							
		0,509	2,86	5,54	14,15	1016,5	2,78	2019-10-14T09:05:52.59364377
		0,482	2,71	5,24	11,17	1027,5	2,81	2019-10-25T09:05:52.59364377
		0,930	5,24	10,13	-14,16	1101,7	3,02	2020-01-07T09:05:52.59364377
NOMINAL MISSION	4							
		0,321	1,81	3,49	16,63	1271,7	3,48	2020-06-25T18:17:34.08000001
		0,284	1,60	3,10	10,79	1278,7	3,50	2020-07-02T18:17:34.08000001
		0,687	3,87	7,48	-16,65	1314,7	3,60	2020-08-07T18:17:34.08000001
	5							
		0,316	1,78	3,44	16,65	1440,7	3,94	2020-12-11T18:17:34.08000001
		0,284	1,60	3,09	11,69	1446,7	3,96	2020-12-17T18:17:34.08000001
		0,682	3,84	7,42	-16,65	1482,0	4,06	2021-01-22T18:17:34.08000001
	6							
		0,321	1,81	3,50	16,62	1608,0	4,40	2021-05-28T18:17:34.08000001
		0,284	1,60	3,10	10,88	1615,0	4,42	2021-06-04T18:17:34.08000001
		0,687	3,86	7,48	-16,65	1651,0	4,52	2021-07-10T18:17:34.08000001
	7							
		0,317	1,78	3,45	16,65	1777,0	4,87	2021-11-13T18:17:34.08000001
		0,284	1,60	3,09	11,78	1783,0	4,88	2021-11-19T18:17:34.08000001
		0,683	3,84	7,43	-16,65	1819,0	4,98	2021-12-25T21:14:42.18062932
	8							
		0,356	2,00	3,87	24,82	1948,2	5,33	2022-05-03T20:45:51.98334052
		0,324	1,83	3,53	17,50	1955,2	5,35	2022-05-10T20:45:51.98334052
		0,688	3,87	7,49	-24,84	1995,2	5,46	2022-06-19T20:45:51.98334045
	9							
		0,360	2,03	3,92	24,84	2116,2	5,79	2022-10-18T20:45:51.98334045
		0,324	1,83	3,53	16,53	2124,2	5,82	2022-10-26T20:45:51.98334045
		0,692	3,89	7,53	-24,84	2164,2	5,93	2022-12-05T20:45:51.98334045
	10							
		0,356	2,01	3,88	24,83	2285,5	6,26	2023-04-05T20:45:51.98334045
		0,324	1,83	3,53	17,60	2292,5	6,28	2023-04-12T20:45:51.98334045
		0,688	3,87	7,49	-24,84	2332,5	6,39	2023-05-22T20:45:51.98334045
	11							
		0,361	2,03	3,93	24,84	2453,5	6,72	2023-09-20T20:45:51.98334045
		0,324	1,83	3,53	16,64	2461,5	6,74	2023-09-28T20:45:51.98334045
		0,689	3,88	7,50	-24,84	2501,5	6,85	2023-11-07T13:10:09.21230169

Table 5: field of views of the METIS coronagraph during the cruise and nominal phases of Solar Orbiter mission for a launch date in 2017. Latitudes in this Table refer to the Solar Orbiter spacecraft heliolatitudes.

The spatial resolution (in km/pixel) of the METIS coronagraph will change over the whole mission, as the Solar Orbiter spacecraft will get closer or farther from the Sun. As it is shown in Table 5, if one considers the first two orbits of the nominal mission, it turns out that for typical spacecraft's heliocentric distances of 0.28 AU (observations at perihelium), 0.32 and 0.68 AU (observations at higher and lower helio-latitudes), the instrument field of view intervals will be between 1.6-3.1 R_{sun} ,1.8-3.5 R_{sun} and 3.9-7.5 R_{sun} respectively, corresponding to spatial resolutions of about 4100 km/2pix, 4600 km/2pix, and 9900 km/2pix respectively. With typical CME speeds given above, this implies that the CME front will leave the METIS FOV in ~ 500-1000 sec at 0.28-0.32 AU and in ~ 1000-2000 sec at 0.68 AU.

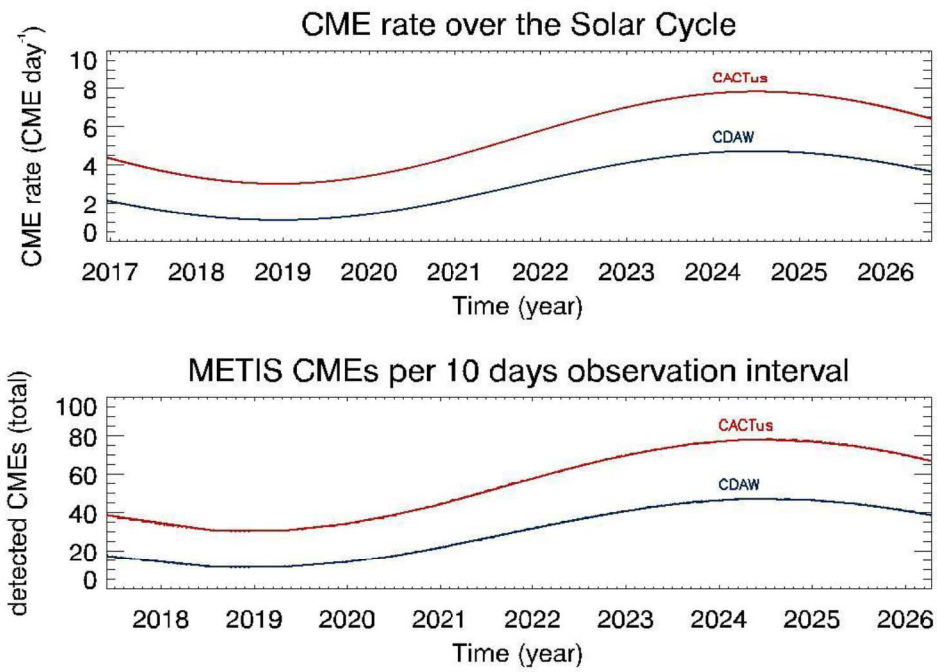

Figure 6: expected CME rates (events/day) during the first years of Solar Orbiter mission as provided by the CACTus and CDAW CME catalogues.

Statistical studies showed that the average CME speed is correlated with the CME rate following the solar activity cycle (see review by Webb & Howard 2012), as well as the probability of type-II radio burst occurrence. During the first two orbits in the nominal mission METIS will observe the solar corona 3.5 – 4.0 years after launch, hence with a launch date in 2017 these observations will occur between 2020 – 2021, in the rising phase of the next solar activity cycle. Each METIS observation interval will have a duration of about 10 days, for a total of 30 days of observations per orbit, with about two orbits per year. Hence, by assuming typical variations of CME rate as determined from the CACTus (Robbrecht et al. 2009) and CDAW (Gopalswamy et al. 2005) catalogues, about 20 – 40 CMEs are expected during every 10 day observation interval. This means that during the first 2 orbits no more than ~ 2-4 CMEs per day are expected, hence once the CME mode is activated it should last for at least ~ half a day in order to be sure to detect at least one CME.

4. Requirements for METIS CME observation mode

In this paragraph the above observational properties of CMEs are taken into account in order to summarize the main requirements to optimize CME observations with METIS coronagraph[4].

4.1 Constraints on the exposure times

Constraints given by the S/N ratio:

- WL: in order to have a S/N ratio > 10 on the pB (combination of 4 exposures) the minimum exposure time is 5 sec (on the single exposure) – based on the streamer intensities at solar minimum.

- UV: in order to have a S/N ratio ~ 10 the minimum exposure time is 40 sec – based on the streamer intensities at solar minimum (30 sec for streamers at solar maximum).

Constraints given by the CME motion (on the plane of the sky):

- WL: by assuming CME speed between 1200-2200 km/s (lower and upper limits for CME associated with type-II radio burst and WL shock signature), with METIS resolutions by 4100-9900 km/2pix (first 2 orbits) exposure times on the order of ~ 2-8 sec are required.

- UV: same constraint as for the WL.

Constraints given by the CME peak brightness:

- WL: during CMEs the WL total brightness increases only by 30%-40%, hence with exposure times for coronal observations (5 sec) we expect no image saturation.

- UV: the HI Lya intensity is comparable with that of coronal streamers at solar maximum, hence with exposure times for coronal observations (30-40 sec) we expect no image saturation.

CONCLUSION

Suggested single exposure times are 10 sec for WL, 40 sec for UV.

4.2 Constraints on the time cadence

Constraints given by experiences on other coronagraphs:

- SOHO-LASCO/C2: typical time cadence is 24 min (for tB), with exposure time by 25 sec. This time cadence is far too large for faster CMEs observed by METIS, because the CME front will leave the METIS FOV in ~ 500-1000 sec at 0.28-0.32 AU and in ~ 1000-2000 sec at 0.68 AU, hence with this cadence the front will fall in the instrument FOV over only 1-2 exposures. Single exposure time is very large: with a resolution by 8260 km/pix a fast CME (2000 km/s) will cross ~ 6 pixels in the exposure time, resulting in a significant blurring of the single CME image.

- STEREO-COR1: typical time cadence is 5 min (for pB), with single exposure time by 1.7 sec (for a single polarized image, 3 polarized images are acquired in sequence with a cadence by 9 sec). This cadence time is the maximum possible for METIS, because the CME front will leave the METIS FOV in ~ 500-1000 sec at 0.28-0.32 AU and in ~ 1000-2000 sec at 0.68 AU, hence with this cadence the

[4] *All the information provided here were already shown and discussed with the METIS PO with a ppt presentation given on 13/02/2013.*

front will fall in the instrument FOV over only 2-6 exposures. Single exposure time is optimized for fast CMEs: with a resolution by 2720 km/pix a fast CME (2000 km/s) will cross ~ 1.2 pixels in the exposure time, hence no blurring at all of the single CME image.

CONCLUSION

Suggested time cadence should be better than 5 min.

4.3 Constraints on the total duration of the observing mode

Constraints given by experiences with previous observations:

- CME origin: SXR brightnenings are observed 15-30 minutes before the eruption; slow rise of prominences starts 5-7 hours before the eruption; high-rate type-III radio bursts are observed 5-10 hours before the eruption; new flux emergences begin a few days before the eruption; pre-CME blobs propagating nearby streamers are observed a few days before the eruption. (P. F. Chen *Living Rev. Solar Phys.* 8, 2011, 1)

- CME expansion: in order to observe the whole event and the beginning of post-CME reconfiguration (e.g. post-CME current sheet) a minimum of ~ 5-6 hours of data after CME initiation (trigger) are required.

CONCLUSIONS

Suggested total duration should be not less than 5-6 hours after CME initiation or CME flag. Study of CME origin would require at least additional 5-10 hours of observations before the CME.

4.4 Constraints given by METIS instrumental parameters and Solar Orbiter telemetry

The main determining parameters are:

Image sizes:	WL images are (2048×2048 pixels)×16 bit = 67.1 Mbit
	UV images are (2048×2048 pixels)×14 bit = 58.7 Mbit
Image compression factor:	assumed equal to 10
Telemetry limit:	27 Gbit/orbit = 27 Gbit / 30 days
Full pB sequence time:	4 images × 10 seconds = 40 seconds
Full pB sequence size compressed:	4 images × 67.1 Mbit / 10 = 26.8 Mbit
UV image time:	1 image × 40 seconds = 40 seconds
UV image size compressed:	1 image × 58.7 Mbit / 10 = 5.9 Mbit

Hence the maximum allowed number of full pB sequences over 30 days will be given by 27 Gbit / 26.8 Mbit = 1007 sequences / 30 days ~ 1.4 sequences/hour (cadence: 43 minutes). This could be a possible WL baseline sequence. On the other hand, the maximum allowed number of UV images over 30 days will be given by 27 Gbit / 5.9 Mbit = 4576 images / 30 days ~ 6.3 images/hour (cadence: 9.5 minutes). This could be a possible UV baseline sequence. This means that the maximum allowed number of pB sequence + UV images over 30 days will be 27 Gbit / (26.8 + 5.9) Mbit = 825 pB + UV sequences / 30 days ~ 1.1 sequences/hour (cadence: 52 minutes). This could be a good example of possible WL+UV baseline sequence.

5. Summary and conclusions

Given all the above constraints, possible CME observation sequences could be summarized as follows:

- **Example of possible CME WL sequence (triggered by a CME flag):** Single WL exposure time: 10 sec; WL cadence: 2 min; WL total duration: 6 hours → 180 full pB sequences corresponding to **~ 4.8 Gbit** (compressed).

- **Example of possible CME UV sequence (triggered by a CME flag):** Single UV exposure time: 40 sec; UV cadence: 1 min; UV total duration: 6 hours → 360 UV images corresponding to **~ 2.1 Gbit** (compressed).

- **Example of possible CME WL + UV sequence (triggered by a CME flag):** Single WL exposure time: 10 sec; single UV exposure time: 40 sec; WL+UV sequence cadence: 3 min; total duration: 6 hours → 120 full pB sequences + 120 UV images, corresponding to ~ 3.2 Gbit + 0.7 Gbit = **3.9 Gbit** (compressed).

With the above CME observation sequences, possible CME campaigns with METIS could be:

- **Example of possible CME WL campaign (for CME monitoring, 2-4 CMEs/day expected):** Single WL exposure time: 10 sec; WL cadence: 4 min; WL total duration: 24 hours → 360 full pB sequences corresponding to **~ 9.6 Gbit** (compressed).

- **Example of possible CME UV campaign (for CME monitoring, 2-4 CMEs/day expected):** Single UV exposure time: 40 sec; UV cadence: 2 min; UV total duration: 24 hours → 720 UV images corresponding to **~ 4.2 Gbit** (compressed).

- **Example of possible CME WL + UV campaign (for CME monitoring, 2-4 CMEs/day expected):** Single WL exposure time: 10 sec; single UV exposure time: 40 sec; WL+UV sequence cadence: 5 min; total duration: 24 hours → 288 full pB sequences + 288 UV images, corresponding to ~ 7.7 Gbit + 1.7 Gbit = **9.4 Gbit** (compressed).

- **Example of possible CME WL campaign (for CME origin and post-CME reconfiguration studies):** Single WL exposure time: 10 sec; WL cadence: 4 min; WL total duration: 48 hours → 720 full pB sequences corresponding to **~ 19.2 Gbit** (compressed).

- **Example of possible CME UV campaign (for CME origin and post-CME reconfiguration studies):** Single UV exposure time: 40 sec; UV cadence: 2 min; UV total duration: 48 hours → 1440 UV images corresponding to **~ 8.4 Gbit** (compressed).

- **Example of possible CME WL + UV campaign (for CME origin and post-CME reconfiguration studies):** Single WL exposure time: 10 sec; single UV exposure time: 40 sec; WL+UV sequence cadence: 5 min; total duration: 48 hours → 576 full pB sequences + 576 UV images, corresponding to ~ 15.4 + 3.4 Gbit = **18.8 Gbit** (compressed).

References

Ciaravella, A., Raymond, J.C., van Ballegooijen, A., et al. 2003, ApJ, 597, 1118

Giordano, S., Ciaravella, A., Raymond, J.C., et al. 2013, JGR, 118, 967

Gopalswamy, N., Yashiro, S., Liu, Y., et al. 2005, JGR, 110, A09S15

Gopalswamy, N. 2010, Proc. of the 20th Slovak National Solar Physics Workshop, ed. I. Dorotovic, Slovak Central Observatory, 108

Lin, J., Ko, Y.-K., Sui, L., et al. 2005, ApJ, 622, 1251

Ontiveros, V., & Vourlidas, A. 2009, ApJ, 693, 267

Robbrecht, E., Berghmans, D., & Van der Linen, R.A.M. 2009, ApJ, 691, 1222

Webb, D.F., & Howard, T.A. 2012, Liv. Rev. SP, 9 , 3